Pattern Competition Leads to Chaos

S. Ciliberto[a] and J. P. Gollub
Department of Physics, Haverford College, Haverford, Pennsylvania 19041, and Department of Physics, University of Pennsylvania, Philadelphia, Pennsylvania 19104
(Received 23 December 1983)

Pattern competition has been studied experimentally in the free surface modes of a circular fluid layer that is forced vertically. Interaction between nearly degenerate modes of different symmetry gives rise to periodic and chaotic fluctuations. The time-dependent mode amplitudes have been measured with digital imaging methods. Many of the observed phenomena can be explained by a low-dimensional coupled oscillator model that is related to the Navier-Stokes equations.

PACS numbers: 47.20.+m, 03.40.Gc, 47.35.+i

Some hydrodynamic systems, such as Rayleigh-Bénard convection in a layer whose lateral dimensions are sufficiently small, or Couette-Taylor flow in a system whose vertical height is not too great, are known to have chaotic states that can be described by few-dimensional strange attractors.[1-3] Unfortunately, the physical origin of the chaotic behavior in these systems is still unclear, and predictive models are not generally available. In this paper we report experiments in which chaotic behavior clearly arises from a simple mechanism, competition between two different spatial modes or patterns. We suggest a phenomenological model that is related to the Navier-Stokes equations and explains many of the observations. We also demonstrate that the time-dependent mode amplitudes can be obtained by digital imaging methods, even when several modes are present.

The system of interest is a cylindrical fluid layer in a container that is subjected to a small vertical oscillation. This system was first studied experimentally by Faraday,[4] and the primary instability was explained in an inviscid linearized approximation by Benjamin and Ursell.[5] Although there have been several recent experimental studies[6,7] of the dynamics of this system, the interaction between different spatial patterns has not received quantitative study. It is well known that if the driving amplitude exceeds a critical value $A_c(\nu)$ which is a function of frequency, the free surface develops a pattern of standing waves. The surface deformation $S(r,\theta,t)$ can then be written as a superposition of normal modes

$$S(r,\theta,t)=\sum_{l,m} a_{l,m}(t) J_l(k_{l,m} r)\cos(l\theta),$$

where J_l are Bessel functions of order l and the allowed wave numbers $k_{l,m}$ are determined by the boundary condition that the derivative $J_l'(k_{l,m}R)=0$, where R is the radius of the cylinder. The modes may be labeled by the indices l (giving the number of angular maxima) and m (related to the number of nodal circles). The mode amplitude $a_{l,m}(t)$ develops an instability when the corresponding eigenfrequency (given by the dispersion law for capillary-gravity waves) is approximately in resonance with half the driving frequency ν, and A exceeds A_c. This parametric instability leads to standing waves in which the mode amplitude oscillates at $\frac{1}{2}\nu$.

In our experiments, the container ($R=6.35$ cm) is mounted on the cone of a loudspeaker oscillating accurately in the vertical direction, and the fluid is water of depth 1 cm. Surface wave patterns are studied by refraction: An expanded parallel laser beam traverses the cell vertically and impinges on a translucent screen located 9 cm above the fluid surface. The intensity field on the screen is converted to an analog signal by a vidicon camera and then digitized in $\frac{1}{60}$ s (with a resolution of 320 by 240 points, and 8-bit precision) with use of a fast analog-to-digital converter and frame store residing on a computer bus. We synchronize the digitization with the forcing to insure a constant phase relative to the fundamental oscillation at $\frac{1}{2}\nu$ (typically 7–10 Hz). This allows us to study the *slowly varying parts* of the mode amplitudes, which we denote by $a_l^0(t)$. We omit the second subscript because in practice only a single value of m is significant for a given value of l.

Examples of digitized optical intensity fields formed by stable patterns involving only a single mode (and possibly harmonics) are shown in Fig. 1 for the (7,2) and (4,3) modes. The index l is obvious from the symmetry, while m was determined by matching the frequency to the known dispersion law. (The accuracy of the calculated and observed

FIG. 1. Digitized optical intensity patterns for the (4,3) and (7,2) modes, respectively. The first index gives the number of angular maxima.

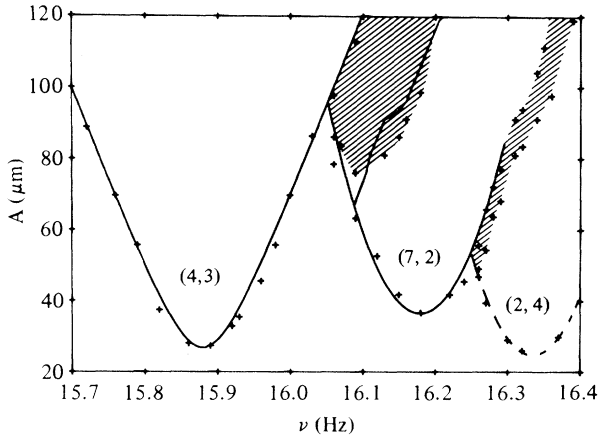

FIG. 2. Portion of the phase diagram as a function of driving amplitude A and frequency ν. Stable patterns occur in the regions labeled by (l,m). Slow periodic and chaotic oscillations occur in the cross-hatched regions. The solid curves are the predictions of a phenomenological mode-coupling model (see text). The crosses are experimental measurements of the phase boundaries.

frequencies is sufficient to eliminate any ambiguity in m.) The white areas correspond to surface depressions (typically about 0.5 mm), and the black ones to surface elevations. The driving amplitude A was about $1.1A_c$ and the frequency was at the minimum of the stability curve in each case. We have observed at least 30 distinct modes with l and m between 1 and 7.

A *small part* of the phase diagram of the system as a function of A and ν is shown in Fig. 2. There are three nearly degenerate modes separated by only about 0.2 Hz. The parabolic curves show the critical amplitude $A_c(\nu)$ for the labeled modes. Below these curves, the surface is nearly flat (except for a small response at the driving frequency). Above but near the minimum of each curve, the motion is dominated by a single mode, and the pattern is stationary. Pattern competition takes place in regions close to the intersections of two stability curves. In these regions, we find that *both* of the neighboring amplitudes are nonzero *and* that they oscillate periodically or chaotically at a mean frequency that is more than two orders of magnitude smaller than ν. We have made a detailed study of the slow variations by digital imaging and spatial Fourier analysis.

We proceed by first integrating the digitized light intensity field over radial segments to reduce noise. We then obtain the relative contributions of different values of l by calculating the magnitude squared of the complex Fourier series for the resulting angular intensity function $\tilde{I}(\theta)$. The height of this "angular power spectrum" $P(l)$ at given l is approximately proportional[8] to the square of the mode amplitude $a_l^0(t)$. (The constants of proportionality depend on radial integrals of the J_l.) Although it is possible to do a two-dimensional normal-mode analysis in both the angular and radial variables, this dramatically increases computational time without providing additional insight.

An example of the angular intensity function $\tilde{I}(\theta)$ and corresponding angular spectrum $P(l)$ for the competition between $l=7$ and $l=4$ modes is shown in Fig. 3. There are seven angular maxima, and the dominant spectral peaks are at $l=7$ and $l=14$. However, there is also a small peak at $l=4$ corresponding to the admixture of a small amount of this mode into the surface displacement. In the regime of pattern competition, we find that the heights of the peaks are time dependent. By doing angular Fourier analysis at many times and plotting the square roots of the spectral heights $P(7)$ and $P(4)$, we obtain (Fig. 4) the time dependence of the mode amplitudes a_7^0 and a_4^0. The slow oscillation resulting from mode competition is periodic in this case, and a_7^0 leads a_4^0 by about 90°. This phase relationship is significant; it implies that (7,2)

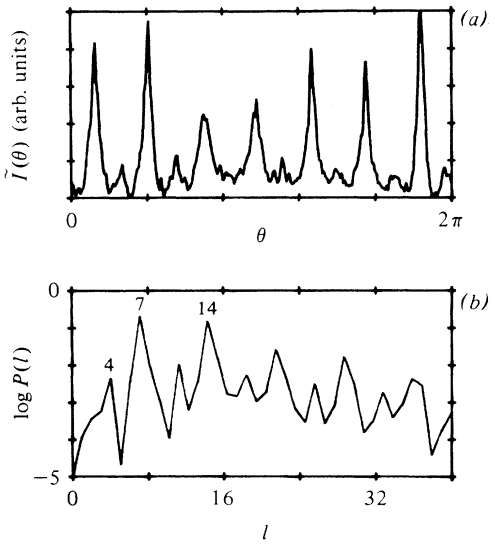

FIG. 3. Angular intensity pattern $\tilde{I}(\theta)$ and corresponding angular spectrum $P(l)$ for a state in which $l=7$ and $l=4$ modes are both present ($A=99$ μm and $\nu=16.113$ Hz). The relative peak heights in the angular spectrum oscillate slowly.

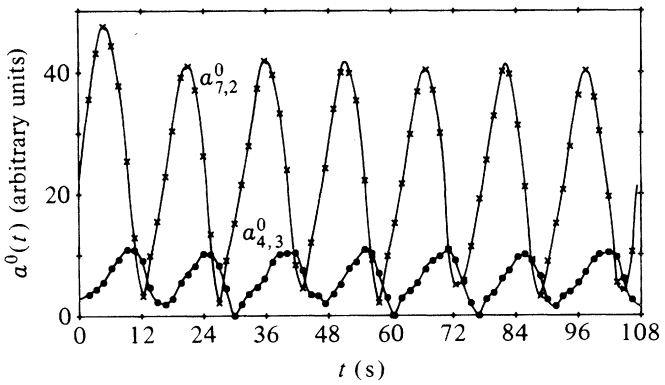

FIG. 4. Time dependence of the slowly varying mode amplitudes $a_4^0(t)$ and $a_7^0(t)$ for $A=99$ μm and $\nu=16.113$ Hz. Chaotic oscillations are found at lower driving frequencies.

pumps (4,3).

The properties of the slow oscillation vary as one traverses the cross-hatched region of Fig. 2. Most importantly, a small reduction in driving frequency (to the left third of the large shaded region of Fig. 2) leads to chaotic oscillations that clearly have broadband frequency spectra. We have observed a period-doubling bifurcation, but cannot yet say if there is a complete sequence of period doublings. A thorough study of the bifurcation structure of this system will require better stability in the fluid properties than we have so far achieved, because the entire regime of mode competition has a width in ν that is less than 1% of ν.

We have constructed a simple phenomenological model whose form is motivated by the fact that in a linearized inviscid approximation to the Navier-Stokes equations, each mode amplitude follows a forced Mathieu equation.[5] We introduce damping, nonlinearity (to prevent divergence), and mode coupling to obtain for each mode

$$\ddot{a}_l+\gamma_l\dot{a}_l+(\omega_l^2-\psi_l A\cos 2\pi\nu t)a_l=\zeta_l a_l^3,$$

where ω_l is the eigenfrequency, γ_l is a damping coefficient that determines the critical threshold $A_c(\nu)$, ζ_l is the coefficient of the cubic term that limits the growth of the mode, and ψ_l is the gain coefficient of the forcing term. In order to describe the interactions between modes, we assume that the gain coefficients are coupled. For example, to describe the interaction of the $l=4$ and $l=7$ modes, we set

$$\psi_4=\bar{\psi}_4+\beta_{47}a_7^2 \text{ and } \psi_7=\bar{\psi}_7+\beta_{74}a_4^2,$$

where the coupling coefficients β_{47} and β_{74} have opposite signs. (Other coupling schemes may also produce sensible results.) Finally, we use the fact that the time scales are widely separate to express the mode amplitudes in terms of slowly varying functions $C_l(t)$ and $B_l(t)$:

$$a_l(t)=C_l(t)\cos(\pi\nu t)+B_l(t)\sin(\pi\nu t).$$

[The *measured* amplitudes $a_l^0(t)$ result from sampling at a fixed phase with respect to the fast oscillation, and are hence linear combinations of C_l and B_l.] Now the coefficients γ_l and $\bar{\psi}_l$ are adjusted to fit the stability curves and the nonlinear coefficients ζ_l are chosen to obtain the correct saturation amplitudes, all in a region where only a *single mode* is present. We numerically integrate the resulting four-dimensional system for the slow variables C_7, B_7, C_4, and B_4, and find that regenerative oscillations (both periodic and chaotic) are in fact produced in the interaction region. We adjust the two mode-coupling coefficients to obtain an oscillatory domain similar in size to that found in the experiments. The predicted phase boundaries are the *solid lines* in Fig. 2. A detailed study of the bifurcation structure of this nonlinear model will be presented elsewhere.[9] It resembles in some respects the forced spherical pendulum, a four-dimensional system that has been discussed recently by Miles.[10]

Finally, we show in Fig. 5 the mean period of the slow oscillations as a function of frequency as one

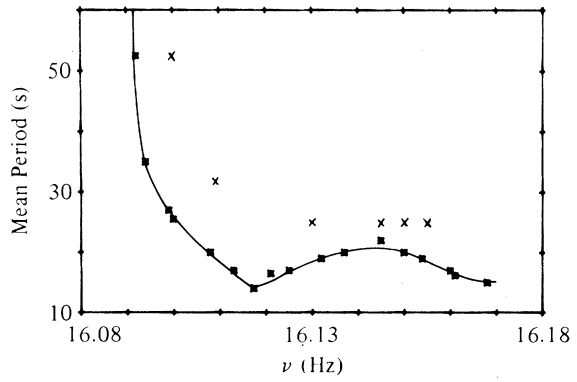

FIG. 5. Mean period of the regenerative oscillation as a function of driving frequency for $A = 99$ μm. Solid points are experimental, and crosses are obtained from the model.

crosses the 0.1-Hz wide interaction region. The solid points are experimental data, while the crosses are the results of the numerical model. We do not show numerical results below 16.10 Hz because the frequency spectrum is extremely broad in that region. The numerical results for the period and its dependence on frequency are roughly correct and could be improved further by tuning the model.

Summarizing, we have shown that the interaction of two modes with different symmetries gives rise to slow oscillations and chaos, and have described a coupled oscillator model whose form is suggested in part by the hydrodynamic equations. We believe that pattern competition might well be a fairly common source of chaos.

This work was supported by Grants No. MEA-7912150 and No. MEA-8310933 from the National Science Foundation. One of us (S.C.) acknowledges the support of a NATO-Consiglio Nazionale delle Ricerche fellowship. We thank P. Hohenberg, T. Lubensky, and L. Narducci for helpful discussions.

[a]Permanent address: Istituto Nazionale di Ottica, Florence, Italy.

[1]B. Malraison, P. Atten, P. Bergé, and M. Dubois, J. Phys. (Paris), Lett. 44, L-897 (1983).

[2]A. Brandstater, J. Swift, H. L. Swinney, A. Wolf, J. D. Farmer, E. Jen, and P. J. Crutchfield, Phys. Rev. Lett. 51, 1442 (1983).

[3]J. Guckenheimer and G. Buzyna, Phys. Rev. Lett. 51, 1438 (1983).

[4]M. Faraday, Philos. Trans. Roy. Soc. London 299, 319 (1831).

[5]T. B. Benjamin and F. Ursell, Proc. Roy. Soc. London, Ser. A 225, 505 (1954).

[6]J. P. Gollub and C. W. Meyer, Physica (Utrecht) 6D, 337 (1983).

[7]R. Keolian, L. A. Turkevich, S. J. Putterman, and I. Rudnick, Phys. Rev. Lett. 47, 1133 (1981).

[8]This assumes that the optical intensity field is linear in the surface wave height, and that only a single value of m is significant for each l. In fact, optical nonlinearity creates extra spatial harmonic content.

[9]Nonlinear models have been used to describe the behavior of a *single* mode by F. T. Dodge, D. D. Kana, and H. N. Abramson, AIAA J. 3, 685 (1965).

[10]J. Miles, to be published.

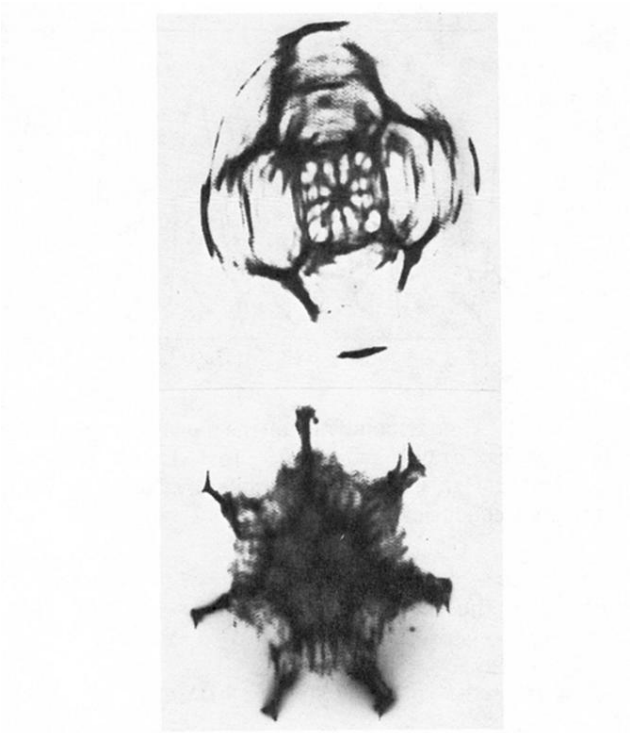

FIG. 1. Digitized optical intensity patterns for the (4,3) and (7,2) modes, respectively. The first index gives the number of angular maxima.